

# Accelerating retreat and high-elevation thinning of glaciers in central Spitsbergen

Jakub Małeckı

## Abstract

Svalbard is a heavily glacier-covered archipelago in the Arctic. Central parts of its largest island, Spitsbergen, are the driest and hence occupied by only small alpine glaciers, for which the post-Little Ice Age response to climate warming remains only sporadically investigated. This study presents a comprehensive analysis of glacier changes in the arid Dickson Land (DL) based on inventories compiled from topographic maps and digital elevation models for the Little Ice Age maximum, the 1960s, 1990 and 2009/11. The  $37.9 \pm 12.1$  % total glacier area decrease in DL was accompanied by increasing annual rates of front retreat over the three study periods. Recently, most of the local glaciers have been consistently thinning in all elevation bands, which is in contrast to larger Svalbard ice masses which remain closer to balance. The mean 1990–2009/11 geodetic mass balance of glaciers in DL is among the most negative from the Svalbard regional means known from the literature. Its application to all central Spitsbergen yields an estimate of a post-1990 sea-level rise input of  $0.6 \text{ Gt a}^{-1}$ , which is considerable given the low glacier-cover of the region.

## 1 Introduction

Small glaciers are natural indicators of climate, as they record even slight oscillations via changes of their thickness, length and area (Oerlemans, 2005). Twentieth century climate warming caused a volume loss of ice masses on a global scale (IPCC, 2013), contributing to about half of the recent rates of sea-level rise. Despite the relatively small area of glaciers and ice caps, their fresh-water input to sea-level rise is of similar magnitude to that from the largest ice masses in the world: the Antarctic and Greenland ice sheets (Radić and Hock, 2011; Gardner et al., 2013). Therefore, it is of great importance to study the volume changes of all land ice masses on both hemispheres.

The archipelago of Svalbard is one of the most significant arctic repositories of terrestrial ice. Glaciers and ice caps cover 57 % of the islands ( $34 \cdot 10^3 \text{ km}^2$ ) and have a total volume of  $7 \cdot 10^3 \text{ km}^3$  (Nuth et al., 2013; Martín-Español et al., 2015). It is located in close proximity to the warm West Spitsbergen Current and its cryosphere is hence considered very sensitive to changing climatic and oceanic conditions (Hagen et al., 2003). The climate record suggests a sharp, early 20<sup>th</sup> century air temperature increase on Svalbard, terminating the Little Ice Age period (LIA) around the 1920s (Hagen et al., 2003). A cooler period between the 1940s and 1960s was followed by a strongly positive summer temperature trend, i.e.  $0.7^\circ\text{C decade}^{-1}$  for the period 1990–2010 (Førland et al., 2011; James et al., 2012; Nordli et al., 2014). Climate warming led to volume loss of the Svalbard glaciers (although with large spatial variability), particularly after 1990 (Hagen et al., 2003; Kohler et al., 2007; Sobota, 2007; Nuth et al., 2007; 2010; 2013; Moholdt et al., 2010; James et al., 2012).

Strong climatic gradients over the archipelago are an important factor modifying the response of Svalbard glaciers to climate change. Coastal zones receive the highest precipitation and experience low summer temperature, and hence are heavily glacier-covered. In contrast, the interior of Spitsbergen, the largest island of the archipelago, shows little ice area, because the distance from the open seas limits moisture transport with a simultaneous increase in air

1 temperature during the summer months (Hagen et al., 1993; Nuth et al., 2013; Przybylak et  
2 al., 2014). The response of glaciers to climate change in these districts has been much more  
3 seldom studied, probably because of their presupposed low significance in the contribution to  
4 sea-level rise, but also because small alpine glaciers are difficult to study with satellite  
5 altimetry and regional mass balance models due to their complex relief. Detailed information  
6 on their spatio-temporal mass balance variability could, therefore, be used to test the  
7 Svalbard-wide modelling assessments. Moreover, research on the evolution of these small  
8 glaciers could be of practical interest, since they neighbour the main settlements of Svalbard.  
9 Consequences of their retreat may influence human activity, e.g. due to increased water and  
10 sediment delivery from glacier basins and associated consequences, such as floods and fjord  
11 bathymetry changes (Szczuciński et al., 2009; Rachlewicz, 2009a; Strzelecki et al., 2015a).

12  
13 One of the regions situated the furthest from maritime influences (ca. 100 km) is the poorly  
14 glacier-covered Dickson Land (DL). This paper inventorises all ice masses of DL and  
15 quantifies changes of their geometry since LIA termination. This includes changes of their  
16 area and length, as well as recent volume fluctuations using digital elevation models obtained  
17 from aerial photogrammetry. The aim of this study is to investigate the response of glaciers in  
18 DL to climate change, with particular focus on their recent mass balance and its spatial  
19 variability. The paper also estimates the contribution of small glaciers in central Spitsbergen,  
20 under-represented in the literature, to sea-level rise.

## 21 22 **2 Study area**

23  
24 The study region is located in central Spitsbergen and stretches between 78°27' N–79°10' N  
25 and 15°16' E–17°07' E. Its area is  $1.48 \cdot 10^3 \text{ km}^2$  with a length of ca. 80 km in north-south  
26 direction and a typical width of 20–30 km. For the purpose of the glaciological analysis, DL  
27 was divided into three subregions—south (DL-S), central (DL-C) and north (DL-N) (Fig. 1).  
28 DL-S is the lowest elevated and is dominated by plateau-type mountains, with summits  
29 reaching 500–600 m a.s.l., occupied by small icefields and ice masses plastered along gentle  
30 slopes. DL-C is the subregion with the greatest ice-cover and the largest glaciers, mostly of  
31 valley type, and summits exceeding 1000 m. The mountains in DL-N are even slightly higher  
32 than in the central part, but glaciers (mainly of valley and niche types) are smaller here and  
33 mostly oriented towards the north.

34  
35 The climate of DL shows strong inner-fjord, quasi-continental characteristics, i.e. reduced  
36 precipitation and increased summer air temperature when compared to the coastal regions.  
37 The southernmost inlet of DL is located about 20 km north of Svalbard Lufthavn weather  
38 station (SVL, 15 m a.s.l.) near Longyearbyen town. Between 1981 and 2010, the Norwegian  
39 Meteorological Institute recorded an average annual temperature of  $-5.1^\circ\text{C}$  at SVL, with the  
40 summer (June-August) mean of  $4.9^\circ\text{C}$ , being relatively high for Svalbard. Annual measured  
41 precipitation was 188 mm. In DL-C daily means of sea-level air temperature are very similar  
42 to those at SVL (Rachlewicz and Styszyńska, 2007; Láska et al., 2012). No meteorological  
43 stations are operating in DL-N, but the general climatic pattern suggests it is among the driest  
44 zones in all Svalbard (Hagen et al., 1993).

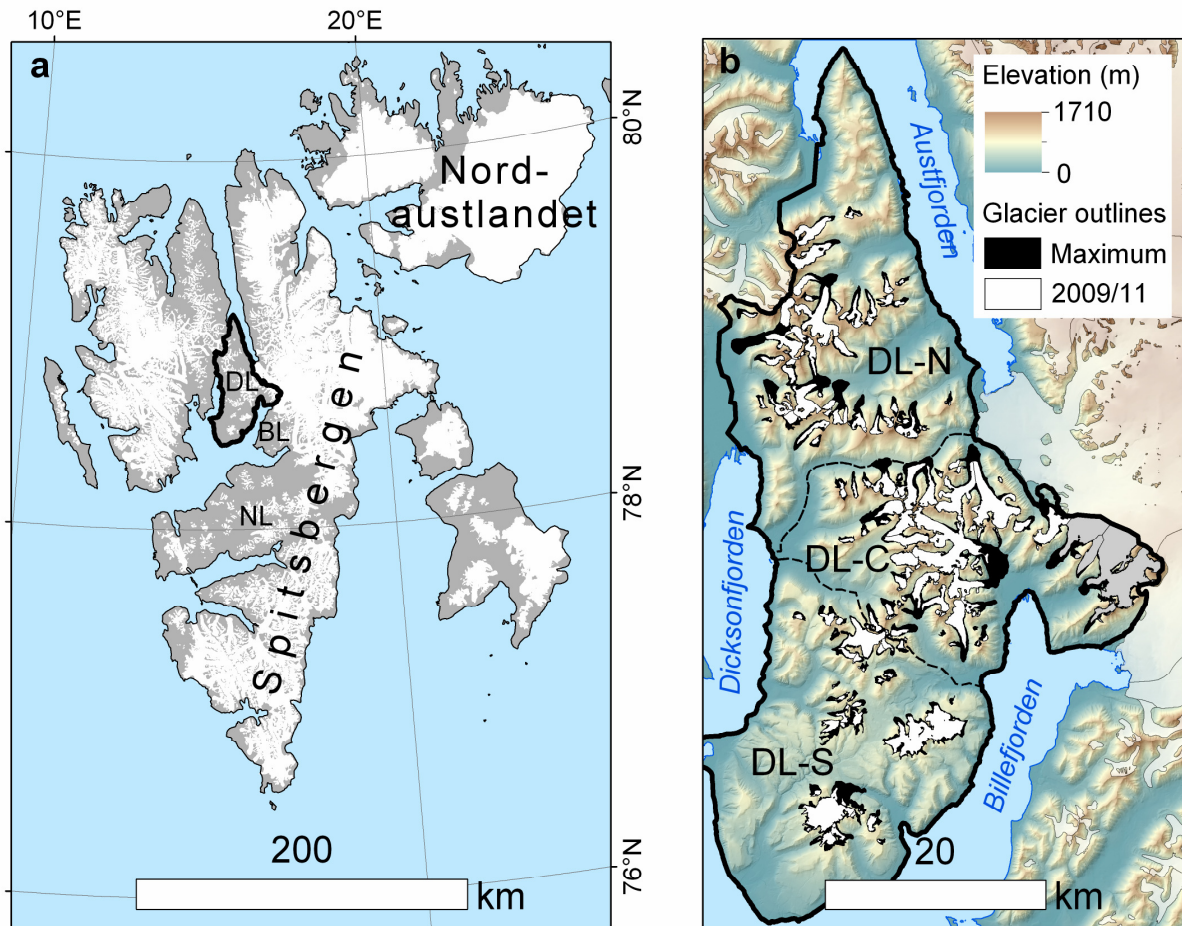


**Fig. 1** Location of the study area. **(a)** Map of Svalbard with locations of regions of central Spitsbergen: Dickson Land (DL), Nordenskiöld Land (NL) and Bünsow Land (BL). **(b)** Map of Dickson Land and its subregions: north (DL-N), central (DL-C) and south (DL-S). Glaciers coloured with grey in the eastern part of DL-C are not covered by 1990 digital elevation model.

Previous glacial research performed in DL-C has focused mainly around the impact of glacier retreat on landscape remodelling (e.g. Karczewski, 1989; Kostrzewski et al., 1989; Gibas et al., 2005; Rachlewicz et al., 2007; Rachlewicz, 2009a,b; Ewertowski et al., 2010; 2012; Ewertowski and Tomczyk, 2015; Evans et al., 2012; Szpikowski et al., 2014; Pleskot, 2015; Strzelecki et al., 2015a,b). More detailed glaciological investigations were performed on Bertilbreen (e.g. Žuravlev et al., 1983; Troicki, 1988) and recently also on Svenbreen (Małecki, 2013a; 2014; 2015). Glaciers in central and eastern parts of DL-C are losing their mass and retreating their fronts (Rachlewicz et al., 2007; Małecki, 2013b; Małecki et al., 2013; Ewertowski, 2014). Glaciers of DL-N and DL-S have not been studied yet.

Glaciers of DL are mostly very small and only the largest ( $>5 \text{ km}^2$ ) are partly warm-based (Małecki, unpublished radar data), so their flow velocities are very low. The maximum ice velocity measured on the largest ice masses of the region does not exceed  $12 \text{ m a}^{-1}$  (Rachlewicz, 2009b), while on smaller glaciers it is several times lower (Małecki, 2014). In every subregion, however, surge-type glaciers occur. Studentbreen, the north-eastern outlet of Frostisen icefield, surged around 1930. Fyrisbreen advanced around 1960 (Hagen et al., 1993) and Hørbyebreen surged probably in the late 19<sup>th</sup> or early 20<sup>th</sup> century (Małecki et al., 2013). Also, visual inspection of 2009/11 aerial imagery by the Norwegian Polar Institute revealed that the Hoegdalsbreen-Arbobreen system, Manchesterbreen and the Vasskilbreen systems are

1 characterised by deformed (looped) flow lines and/or moraines, which may indicate their past  
2 surge behaviour.

### 3 **3 Data and methods**

#### 4 **3.1 Glacier boundaries**

5  
6  
7  
8 A ready-to-use Svalbard glacier geometry product from the Norwegian Polar Institute (NPI)  
9 (König et al., 2013) was evaluated as a potential data source for the purpose of this study. Due  
10 to the large, Svalbard-wide scale of this work, some difficulties were met during preliminary  
11 geometry change analysis. Firstly, many glaciers smaller than 1 km<sup>2</sup> had not been not  
12 catalogued in the NPI database. Secondly, polygons for the 2000s, particularly of the smallest  
13 ice patches, were too coarse to accurately reproduce their subtle decadal changes. Lastly,  
14 based on the author's experience in the study area, it was concluded that many NPI glacier  
15 boundaries tend to include transient snowpatches. Therefore, glacier inventories from this  
16 paper (covering glacier extents from their neoglacial maximum/LIA, 1960s, 1990 and  
17 2009/11) were prepared by the author with the use of the NPI source data, i.e. maps and  
18 modified ice and snow masks.

19  
20 Glacier boundaries for the 1960s were manually digitised using ArcGIS software from  
21 scanned and georeferenced 1:100,000 S100 series paper maps, constructed by NPI from  
22 1:50,000 aerial imagery taken between 1960 and 1966. The LIA area of glaciers was  
23 estimated by adding the area of their moraine zones to the 1960s outlines, but no information  
24 was available for their lateral extent at that time. The 1990 outlines are based on the NPI  
25 glacier database (König et al., 2013), but many polygons were added or modified according to  
26 the author's experience from the field to minimise errors of the final glacier area  
27 measurement. The most recent outlines were taken from the official NPI inventory, which is  
28 based on 2009–2011 aerial photographs (Norwegian Polar Institute 2014a), which proved to  
29 be very accurate during direct field surveys.

30  
31 Confluent glaciers of comparable size separated by a medial moraine were treated as  
32 individual units, except for Ebbabreen, the largest glacier in DL, historically considered as  
33 one object. Where possible, minor tributary glaciers, which eventually separated from the  
34 main stream, were fixed as individual glaciers in the earlier epochs as well, so area changes of  
35 a given glacier result from ice melt-out, rather than from disconnection of former tributaries.  
36 Very small episodic snow fields and elongated snowpatches connected with main glacier  
37 bodies were excluded from the inventory. Ice-divides were fixed in time and did not account  
38 for changing ice topography. The small icefields of Frostisen and Jotunfonna were not further  
39 divided into glacier basins.

#### 40 41 42 **3.2 Digital elevation models**

43  
44 As a 1990 and 2009/11 topographic background for the analysis, 20 m digital elevation  
45 models (DEMs) from the NPI were used (Norwegian Polar Institute, 2014b). The 1990 DEM  
46 was constructed from 1:15,000 aerial photographs and does not cover major glaciers in  
47 eastern DL-C which represent 16.6 % of the modern glacier area of DL (Fig. 1b), so their  
48 elevation changes for the 1990–2009/11 period could not be measured. Data for the most  
49 recent DEM originate from 0.5 m resolution aerial photographs, mainly from 2011, but the  
50 small eastern part of DL was covered by an earlier 2009 campaign. These data sources were

1 projected into a common datum ETRS 1989 and fit into a common cell grid. The universal co-  
 2 registration procedure described by Nuth and Kääb (2011) proved the accurate XYZ  
 3 alignment of both datasets.

### 6 3.3 Calculation of glacier geometry parameters and their changes

8 From the modern boundaries and 2009/11 DEM, the main morphometric characteristics of  
 9 glaciers could be extracted. These were area ( $A$ ), length ( $L$ ), mean slope ( $S$ ), mean aspect ( $\alpha$ ),  
 10 minimum, maximum, median and moraine elevation ( $H_{min}$ ,  $H_{max}$ ,  $H_{med}$  and  $H_{mor}$  respectively)  
 11 and theoretical steady-state equilibrium line altitude ( $tELA$ ), assuming an accumulation area  
 12 ratio of 0.6. The area was measured for each polygon and epoch ( $A_{max}$ ,  $A_{1960}$ ,  $A_{1990}$ ,  $A_{2011}$ ,  
 13 respectively for each of the analysed epochs).  $S$ ,  $\alpha$ ,  $H_{min}$ ,  $H_{max}$  and  $H_{med}$  were computed for  
 14 each polygon for 2009/11.  $L$  was calculated for each epoch along the centrelines of the 66  
 15 largest valley, niche and cirque glaciers, excluding irregular ice masses with no dominant  
 16 flow direction, former minor tributary glaciers that used to share front with the main glacier in  
 17 their basin and very small glaciers with  $A_{max} < 0.5 \text{ km}^2$ . On complex glaciers, e.g. with  
 18 multiple outlets (e.g. Jotunfonna), more than one centerline had to be used to determine the  
 19 representative lengths and retreat rates. Several parameters were used as indicators of glacier  
 20 fluctuations, including area changes ( $dA$ ), length changes ( $dL$ ), volume changes over the  
 21 period 1990–2009/11 ( $dV$ ) and mean elevation change for the period 1990–2009/11 ( $dH$ ), all  
 22 also given as annual rates ( $dA/dt$ ,  $dL/dt$ ,  $dV/dt$  and  $dH/dt$  respectively). All rates of glacier  
 23 change indicators were computed according to the year of validity of geometry data.

25 To compute  $dV$ , elevation change pixel grids were first calculated for each ice mass by  
 26 subtraction of 2009/11 DEM from 1990 DEM. This is an accurate method of mass change  
 27 measurement over long time scales (Cox and March 2004), providing information about  
 28 thickness changes over the entire glacier with no need for extrapolation of mass balance  
 29 values from single reference points, such as the stakes used in the direct glaciological method.  
 30 The arithmetic average of elevation change pixels lying within the larger (here 1990) glacier  
 31 boundary ( $\overline{dh}$ ) was then used to compute  $dV$  using Eq. 1.

$$33 \quad dV = \overline{dh} \cdot A_{1990} \quad (\text{Eq. 1})$$

35 Mean elevation change of glaciers,  $dH$ , was inferred by dividing  $dV$  by the average area of a  
 36 glacier over the period 1990–2009/11 to account for its retreat (Eq. 2).

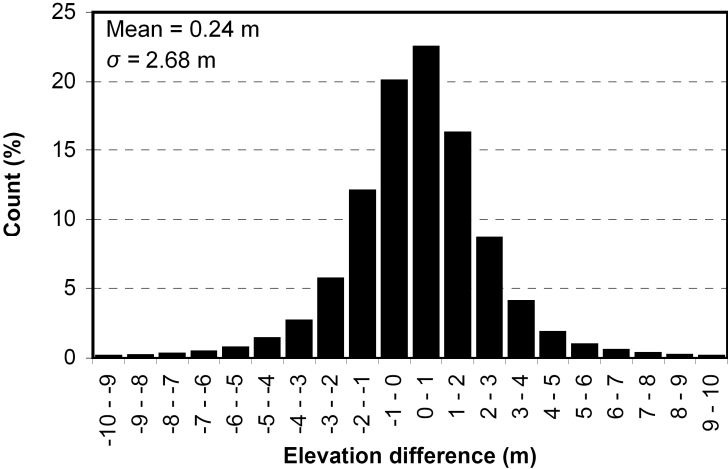
$$38 \quad dH = \frac{2dV}{(A_{1990} + A_{2011})} \quad (\text{Eq. 2})$$

39 Near-surface glacier density changes were not considered in the conversion of the geodetic  
 40 mass balance to water equivalent (w.e.), as they were assumed to be small when compared to  
 41 climatically-induced elevation changes over the study period 1990–2009/11. This assumption  
 42 is more uncertain in the highest zones of glaciers, where changes in firn thickness may lead to  
 43 considerable density variations. However, direct field surveys and analysis of the available  
 44 satellite images indicate that in the late summer the highest glacier zones in DL are usually  
 45 composed of glacier ice or superimposed ice and almost no firn is present. Moreover, Kohler  
 46 et al. (2007) concluded a good match between the geodetic and glaciologically-measured  
 47 cumulative mass balance on a small NW Spitsbergen glacier, implying density changes may  
 48

1 be neglected in geodetic balance calculations on comparatively small and retreating ice  
 2 masses in Svalbard. Therefore,  $dH/dt$  could be converted to water equivalent by multiplication  
 3 by an average ice density of  $900 \text{ kg m}^{-3}$ .

4  
 5  
 6 **3.4 Errors**

7  
 8 Glacier area measurements for the 1960s epoch suffer from errors associated with general  
 9 map accuracy or misinterpretations made by cartographers, e.g. due to the considerable extent  
 10 of winter snow cover on aerial images. To account for that, 25 m was used as a horizontal  
 11 uncertainty of glacier polygon digitalisation. Each polygon was assigned a 25 m buffer with  
 12 "-" and "+" signs. Including these buffers, new areas of DL glaciers were computed and  
 13 compared to all original polygons. Differences between the new and original values were used  
 14 as an error estimate of  $A_{1960}$  for each glacier, with  $\pm 6.4 \%$  as a region-wide total which was  
 15 larger for the smaller ice masses. Since no maps are available for the LIA maximum, LIA  
 16 glacier area estimation is based on the 1960s outlines and geomorphological mapping of  
 17 moraine zones. Such an approach assumes only frontal retreat in the period LIA–1960s, but  
 18 some lateral retreat most likely took place as well. Also, moraine deposits of some glaciers  
 19 could have been either eroded before the aerial photogrammetry era or not formed at all.  
 20 Application of a relatively large  $\pm 50 \text{ m}$  buffer around the LIA outlines resulted in a total  
 21 glacier area error estimate of  $\pm 11.5 \%$  for that epoch. For 1990 and 2009/11 epochs lower  
 22 buffers of  $\pm 10 \text{ m}$  and  $\pm 5 \text{ m}$  were used, resulting in glacier area uncertainty estimates of  $\pm 3.4 \%$   
 23 and  $\pm 2.2 \%$  for the whole DL region. Uncertainties of length measurement for each year  
 24 were set according to the buffers described above.  
 25



26  
 27 **Fig. 2** Histogram of elevation differences between 2009/11 DEM and 1990 DEM over non glacier-covered  
 28 terrain.  
 29  
 30

31 To estimate the error of  $\overline{dh}$  ( $\epsilon$ ) elevation, differences between the 1990 and 2009/11 DEMs  
 32 over non-glacier covered terrain in the whole study region were measured. Since ice surfaces  
 33 in DL are relatively poorly inclined, mountain slopes steeper than  $20^\circ$  were excluded from the  
 34 analysis. The results show that an elevation difference of over 70 % of pixels is within  $\pm 2 \text{ m}$   
 35 and less than 5 % are characterised by an elevation difference of more than  $\pm 5 \text{ m}$  (Fig. 2).  
 36 The mean elevation difference between the two DEMs was 0.24 m, a correction further  
 37 subtracted from all obtained  $\overline{dh}$  values, while the standard deviation,  $\sigma$ , was 2.68 m. Here,  $\sigma$   
 38 is used as a point elevation difference uncertainty and is further used to compute  $\epsilon$  for

1 individual glaciers. The elevation measurement error of snow-covered surfaces was, however,  
 2 expected to be larger than for rocks and vegetated areas due to its lower radiometric contrast  
 3 on aerial images. To account for this effect, parts of glacier surfaces extending above 550 m  
 4 a.s.l. (an approximate snowline on 1990 and 2009/11 aerial imagery) have a prescribed error  
 5 characteristic of  $2\sigma$ . For each glacier,  $\varepsilon$  was then calculated using Eq. (3):  
 6

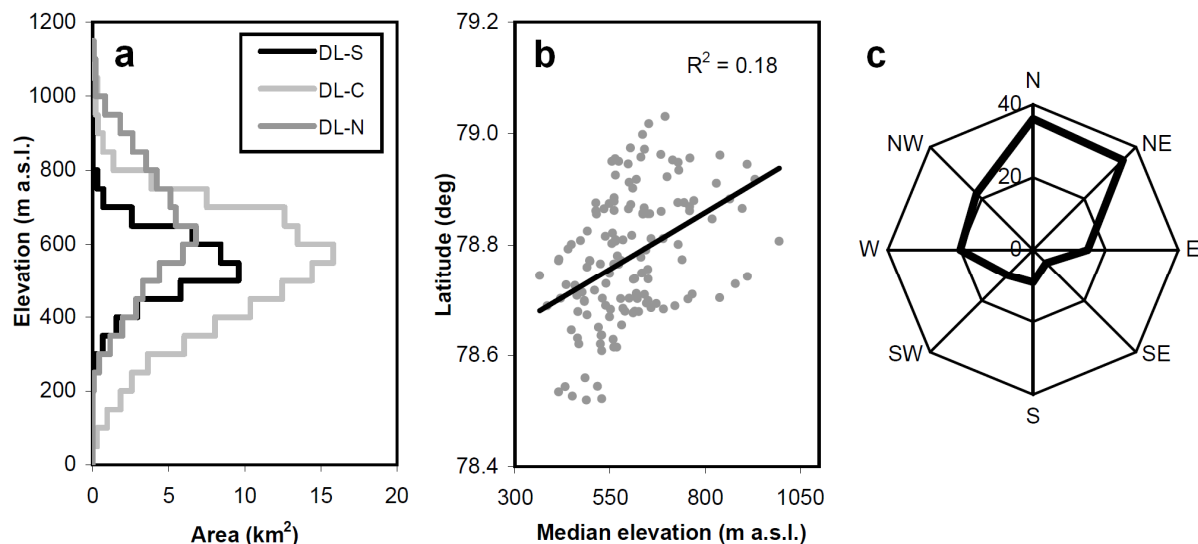
$$7 \quad \varepsilon = \frac{[(1 - n) \cdot \sigma] + (n \cdot 2\sigma)}{\sqrt{N}} \quad (\text{Eq. 3})$$

8  
 9 where  $n$  is the fraction of the glacier extending above 550 m and  $N$  is the sample size.  
 10 Assuming spatial autocorrelation of elevation errors at an order of 1000 m after Nuth et al.  
 11 (2007),  $N$  becomes glacier size in  $\text{km}^2$  rather than number of sample points. Using  $\varepsilon$  and errors  
 12 of glacier area measurements, uncertainties of  $dV$  and  $dH$  could be assessed with conventional  
 13 error propagation methods. All errors are relatively large for the smallest ice masses and *vice*  
 14 *versa*.  
 15  
 16

## 17 4 Results

### 18 4.1 Modern geometry of Dickson Land glaciers

19  
 20  
 21 In the most recent 2009/11 inventory 152 ice masses were catalogued in DL, all terminating  
 22 on the land and covering a total of  $207.4 \pm 4.6 \text{ km}^2$  (14.0 % of the region). 110 ice masses (72  
 23 % of the population) have areas  $< 1 \text{ km}^2$  and 86 of these are smaller than  $0.5 \text{ km}^2$ . Only 9  
 24 glaciers (6 %) are larger than  $5 \text{ km}^2$ . The largest glaciers are Ebbabreen ( $24.3 \text{ km}^2$ ),  
 25 Cambridgebreen-Baliollbreen system ( $16.3 \text{ km}^2$ ), Hørbyebreen system ( $15.9 \text{ km}^2$ ) and  
 26 Jotunfonna ( $14.0 \text{ km}^2$ ). North-facing glaciers (N, NW and NE) comprise 61 % of the  
 27 population, while only 16 % of ice masses have a southern aspect (S, SW and SE). The mean  
 28 glacier slope is  $10.7^\circ$ .  
 29



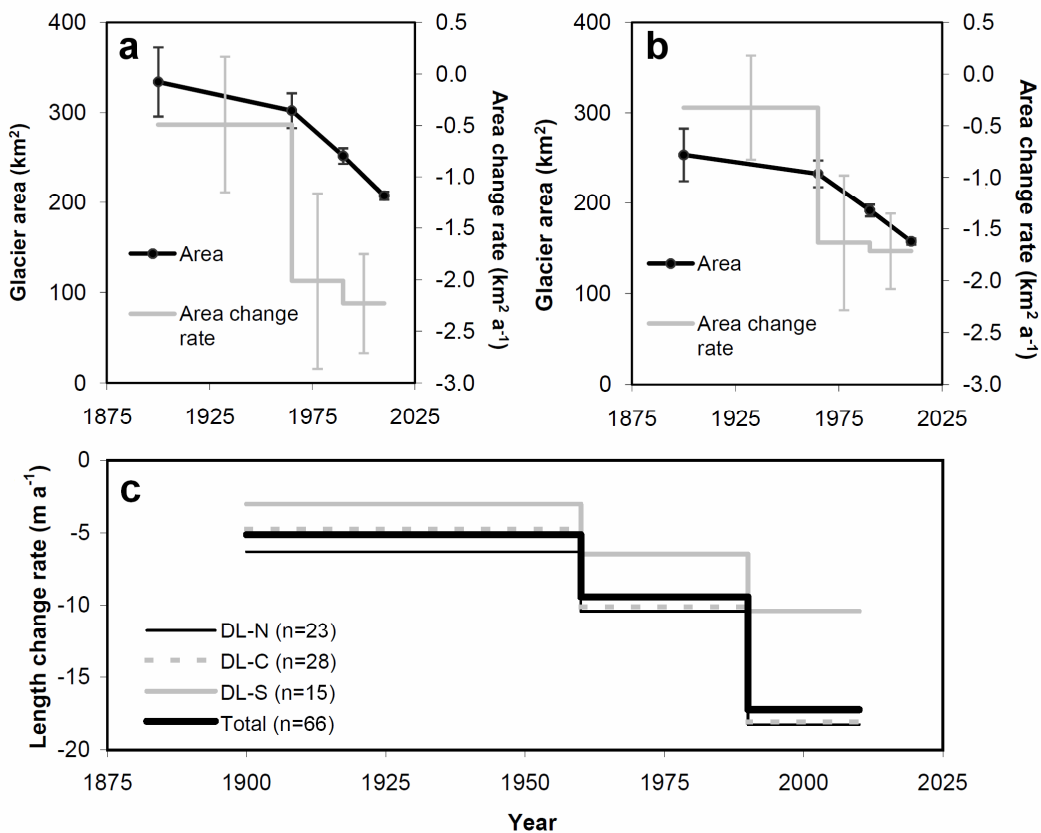
30  
 31  
 32 **Fig. 3** Main features of the modern glacier geometry in DL: area-altitude distribtuion (a), scatter plot of latitude  
 33 against median glacier elevations (b) and frequency distribution of mean glacier aspects (c).  
 34  
 35



1 DL-C is the subregion with the heaviest glacier-cover, at 25.9 % (117.1 km<sup>2</sup>); however this  
 2 cover is only 7.7 % (39.3 km<sup>2</sup>) and 9.8 % (51.0 km<sup>2</sup>) in DL-S and DL-N, respectively. The  
 3 subregions also differ significantly in their area-altitude distribution. The further north, the  
 4 higher the maximum and median glacier elevations, although with a large scatter. DL-N has  
 5 most of the high-elevated glacier area of DL and the median elevation of its glaciers is 614 m.  
 6 In DL-C, glacier fronts reach the lowest elevations, while the glacier hypsometry of DL-S is  
 7 the flattest and contains the lowest fraction of high-elevated areas. The median elevations of  
 8 the two latter subregions are 520 m, giving an overall median elevation of glaciers in DL of  
 9 539 m and a *tELA* of 504 m a.s.l. The total volume of DL ice masses, estimated with  
 10 empirical area-volume scaling parameters by Martín-Español et al. (2015), is roughly 12 km<sup>3</sup>.  
 11 The main details of glacier geometry characteristics are depicted in Fig. 3.

#### 14 4.2 Glacier area and length reduction

16 Since the termination of the LIA, the glaciers of DL have been continuously losing area, in  
 17 total by  $37.9 \pm 12.1$  % (Fig. 4a; Table 1). The overall rate of area loss was  $0.49 \pm 0.66$  km<sup>2</sup> a<sup>-1</sup>  
 18 in the first epoch, which increased fourfold to  $2.01 \pm 0.85$  km<sup>2</sup> a<sup>-1</sup> after 1960 and further to  
 19  $2.23 \pm 0.48$  km<sup>2</sup> a<sup>-1</sup> after 1990 (Fig. 4a). Exclusion of known and probable surge-type  
 20 glaciers, which may change their extent due to internal dynamic instabilities, provides a clear  
 21 insight into the climate-induced area changes in the region and confirms that increasing area  
 22 loss rates are related to climate forcing, rather than ice dynamics (Fig. 4b). The large error  
 23 bars of  $dA/dt$  do not, however, offer a clear picture of the ongoing trend.



25 **Fig. 4 (a)** Changes of the total glacier area in Dickson Land. **(b)** Same as **(a)**, but for non-surging glaciers only.  
 26 **(c)** Average glacier length change rates in Dickson Land and its subregions.  
 27



1

**Table 1** Changing extent of glaciers in Dickson Land over the study periods.

Subregion	Area, $A$ (km <sup>2</sup> )				
	Max	1960s	1990	2009/11	$dA$ Max–2009/11
DL-N	91.76 ± 12.03	78.65 ± 3.35	63.83 ± 2.74	51.05 ± 1.43	–44.4 ± 14.4 %
DL-C	174.95 ± 18.14	159.55 ± 11.81	137.88 ± 4.10	117.07 ± 2.22	–33.1 ± 11.0 %
DL-S	67.40 ± 8.25	63.98 ± 4.17	50.27 ± 1.71	39.32 ± 0.92	–41.7 ± 13.3 %
<b>Total</b>	<b>334.11 ± 38.42</b>	<b>302.18 ± 19.34</b>	<b>251.98 ± 8.57</b>	<b>207.44 ± 4.56</b>	<b>–37.9 ± 12.1 %</b>

2

Subregion	Length change rates, $dL/dt$ (m a <sup>-1</sup> )			
	Max–1960s	1960s–1990	1990–2009/11	Max–2009/11
DL-N (23 glaciers)	–6.3 ± 0.2	–10.4 ± 0.2	–18.3 ± 0.1	–9.5 ± 0.1
DL-C (28 glaciers)	–4.7 ± 0.2	–10.1 ± 0.2	–18.1 ± 0.1	–8.4 ± 0.1
DL-S (15 glaciers)	–3.0 ± 0.2	–6.5 ± 0.3	–10.4 ± 0.1	–5.3 ± 0.1
<b>Total (66 glaciers)</b>	<b>–4.9 ± 0.1</b>	<b>–9.4 ± 0.1</b>	<b>–16.4 ± 0.1</b>	<b>–8.1 ± 0.1</b>

3

4

5 In contrast to  $dA/dt$ , average length change rates  $dL/dt$  suffer from minor uncertainties. From  
6 the available temporal resolution of the data no single front advance was detected, although  
7 the surge events of Frostisen and Fyrisbreen occurred during the first analysed period (Hagen  
8 et al., 1993). In general, all glaciers have been retreating since the LIA termination and the  
9 extremes of total  $dL$  observed in DL were –46 m and –3325 m. Epochs LIA–1960s and  
10 1960s–1990 were the periods of the fastest retreat for only 26 % of the study glaciers. In  
11 many of these cases, bedrock topography supported a short-term boost of  $dL/dt$ , e.g. due to  
12 rock sills dissecting thinning glacier snouts into active and dead ice zones (e.g. Ebbabreen,  
13 Frostisen, Svenbreen). The vast majority of glaciers (74 %) were retreating at their fastest rate  
14 in the last study period 1990–2009/11.

15

### 16 4.3 Glacier thinning and mass balance

17

18

19 A strikingly negative and consistent elevation change pattern is evident from the 1990–2011  
20 data, also in the highest zones of glaciers all over DL (Figs. 5 and 6). At the lowest altitudes  
21 (< 200 m a.s.l.), the mean change rate was ca.  $-2 \text{ m a}^{-1}$ , while at the average  $tELA$  (ca. 500 m  
22 a.s.l.) this was about  $-0.6 \text{ m a}^{-1}$ . Positive fluctuations were observed just above 1000 m a.s.l.  
23 on average, mostly in DL-N. Some glaciers have been thinning at a very high average rate  
24 exceeding  $1 \text{ m a}^{-1}$ , while only a few small ice patches have been closer to balance. Overall,  
25 the average area-weighted  $dH/dt$  in DL was highly negative at  $-0.71 \pm 0.05 \text{ m a}^{-1}$  ( $-0.64 \pm$   
26  $0.05 \text{ m w.e. a}^{-1}$ ), resulting in a total volume loss rate of  $137 \pm 6 \cdot 10^6 \text{ m}^3 \text{ a}^{-1}$  and a mass  
27 balance of  $-0.12 \pm 0.01 \text{ Gt a}^{-1}$  (excluding major glaciers in eastern DL-C due to the lack of  
28 1990 DEM coverage). Subregional values are given in Table 2 and indicate the most negative  
29 specific mass balance to occur in DL-C and the least negative in DL-N.

30

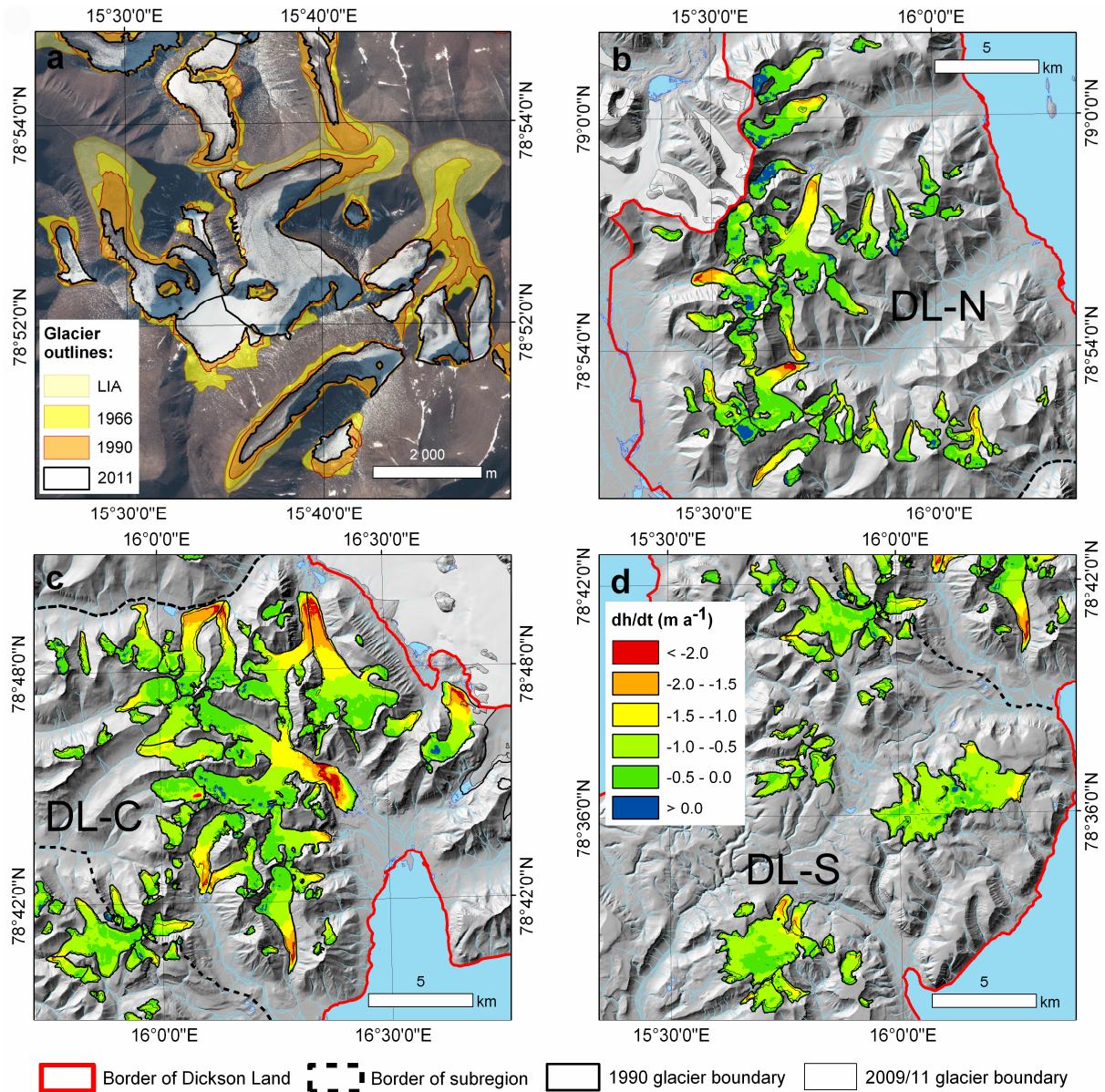
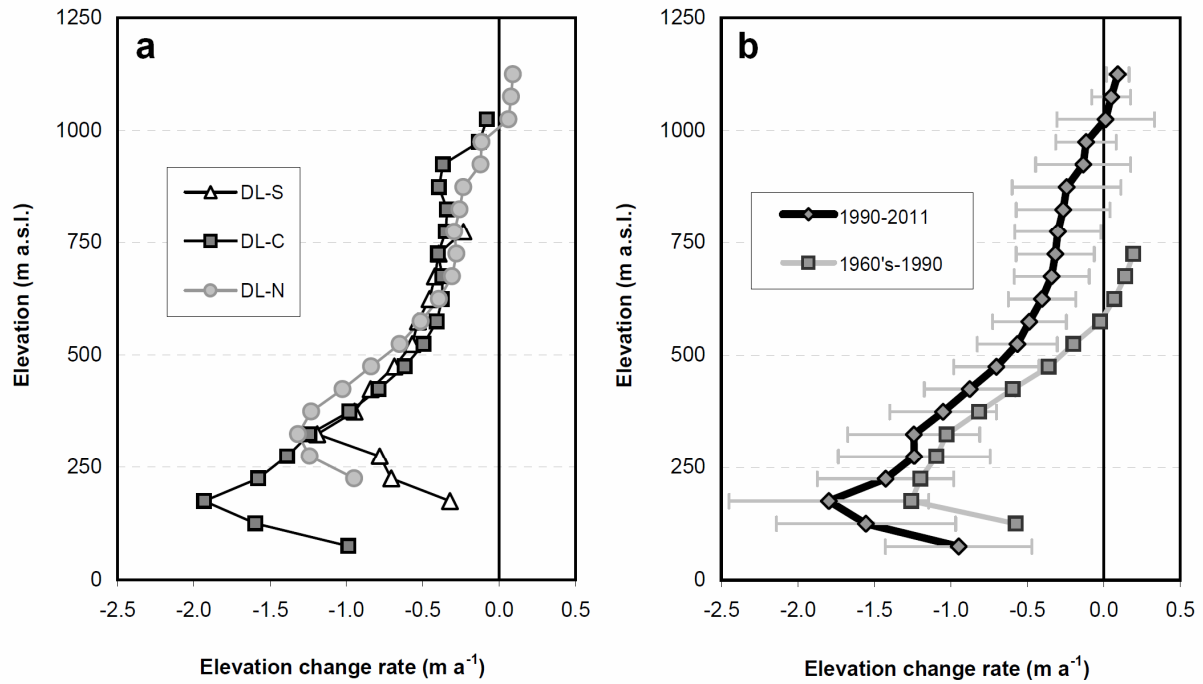


**Fig. 5** An example of glacier area changes in northern Dickson Land in the Vasskillbreen region (a), the mean 1990–2009/11 elevation change rates in northern (b), central (c) and southern (d) Dickson Land. Orthophotomap for (a): ©Norwegian Polar Institute.

**Table 2** Elevation changes, volume changes and mass balance of glaciers in subregions of Dickson Land over the period 1990–2011.

Volume and elevation changes, $dV$ and $dH$ , and their rates $dV/dt$ and $dH/dt$					
Subregion	$dV$ (millions $m^3$ )	$dV/dt$ (millions $m^3 a^{-1}$ )	$dH$ (m)	$dH/dt$ ( $m a^{-1}$ )	Specific mass balance (m w.e.)
DL-N	$-735 \pm 46$	$-35.0 \pm 2.3$	$-12.8 \pm 1.1$	$-0.61 \pm 0.05$	$-0.55 \pm 0.04$
DL-C*	$-1\,482 \pm 67$	$-70.6 \pm 3.3$	$-16.6 \pm 1.2$	$-0.79 \pm 0.06$	$-0.71 \pm 0.05$
DL-S	$-651 \pm 37$	$-31.0 \pm 1.8$	$-14.5 \pm 1.2$	$-0.69 \pm 0.06$	$-0.62 \pm 0.05$
<b>Total*</b>	<b><math>-2\,867 \pm 116</math></b>	<b><math>-136.5 \pm 5.7</math></b>	<b><math>-15.0 \pm 1.0</math></b>	<b><math>-0.71 \pm 0.05</math></b>	<b><math>-0.64 \pm 0.05</math></b>

\*excluding glaciers in eastern DL-C due to the lack of 1990 DEM coverage



1  
2 **Fig. 6 (a)** Homogeneity of the 1990–2009/11 elevation change pattern in DL subregions. **(b)** The mean pre-1990  
3 and post-1990 elevation change rates in DL averaged from the available data. Horizontal bars represent one  
4 standard deviation. The 1960s–1990 data compiled from Małeckı (2013b) and Małeckı et al. (2013).

#### 5 6 7 **4.4 Links between glacier change indicators and their geometry**

8  
9 Recent thinning rates on glaciers have shown a clear trend decreasing with altitude, so the  
10 highest elevated glaciers (mainly in DL-N) have been thinning the slowest, while glaciers  
11 with a large portion of low-elevated ice (e.g. as in DL-C) had the fastest thinning rates (Fig.  
12 7a).  $dL$  was correlated with terminus altitude and glacier length, so low-elevated fronts of  
13 long glaciers have been retreating at the fastest rates. Relative area change was best correlated  
14 with relative length change (Fig. 7b), glacier area, maximum elevation and length, so large  
15 glaciers lost the smallest fraction of their maximum extent despite significant absolute area  
16 and length losses. In contrast to reports from many other regions of the globe (e.g. Li and Li  
17 2014; Fischer et al., 2015; Paul and Mölg 2014), glacier aspect showed no statistical  
18 correlation with any of the glacier change parameters, which may result from the summertime  
19 midnight-sun over Svalbard and the more balanced insolation on slopes with north and south  
20 aspects when compared to mid-latitudes. Pearson correlation coefficients of glacier change  
21 parameters against other parameters and glacier geometry variables are given in Table 3.

22

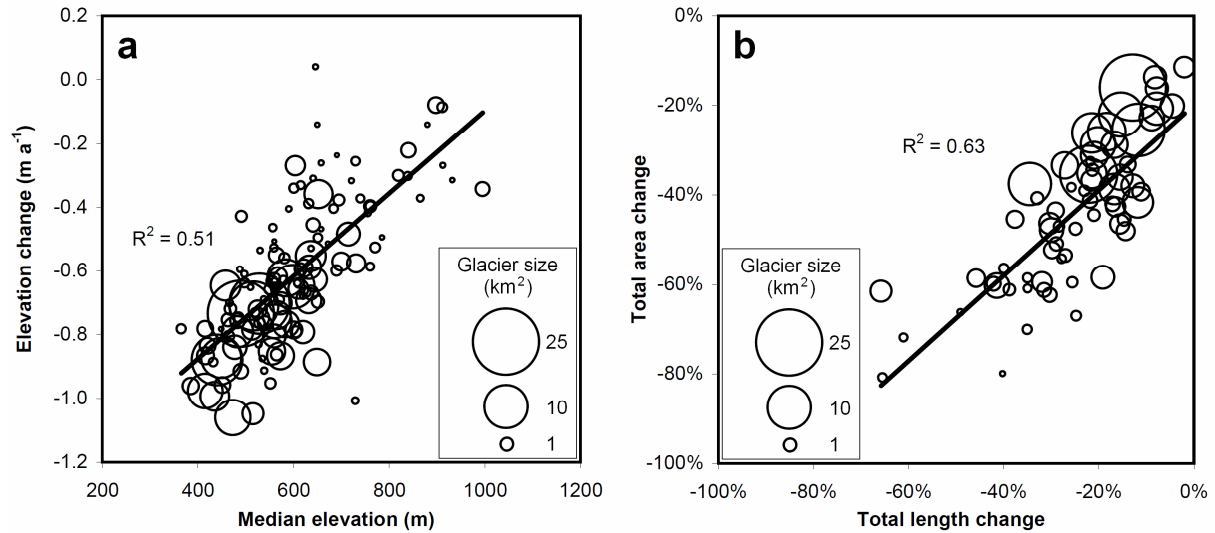


**Fig. 7** Scatter plots showing the relationship between mean 1990–2009/11 glacier elevation change and median elevation of glaciers (a) and total area change and total length change of glaciers (b).

**Table 3** Pearson correlation coefficients for glacier change indicators against other indicators and geometry parameters. Bold values indicate statistical significance at  $p = 0.01$  level.

	$dA$ Max- 2009/11	$dA$ 1990- 2009/11	$dL/dt$ Max- 2009/11	$dL/dt$ 1990- 2009/11	Relative $dL$ Max- 2009/11	Relative $dL$ 1990- 2009/11	$dH/dt$	$\ln(A_{max})$	$\ln(A_{2011})$	$L_{max}$	$L_{2011}$	$H_{med}$	$H_{min}$	$H_{max}$	$H_{mor}$	$tELA$	$S$	$\cos \alpha$	Longitude	Latitude
$dA$ Max-2009/11	1	<b>0.40</b>	0.19	0.13	<b>0.79</b>	<b>0.54</b>	<b>0.21</b>	<b>0.42</b>	<b>0.60</b>	<b>0.47</b>	<b>0.62</b>	<b>0.24</b>	-0.12	<b>0.51</b>	0.03	<b>0.21</b>	<b>-0.31</b>	-0.11	0.14	<b>0.24</b>
$dA$ 1990-2009/11	<b>0.40</b>	1	-0.13	0.17	<b>0.41</b>	<b>0.58</b>	0.08	<b>0.33</b>	<b>0.50</b>	<b>0.49</b>	<b>0.52</b>	0.13	-0.16	<b>0.38</b>	-0.08	0.10	<b>-0.27</b>	0.03	0.09	<b>0.23</b>
$dL/dt$ Max-2009/11	0.19	-0.13	1	<b>0.69</b>	<b>0.50</b>	<b>0.36</b>	0.15	<b>-0.45</b>	<b>-0.36</b>	<b>-0.59</b>	<b>-0.33</b>	0.21	<b>0.57</b>	-0.26	<b>0.73</b>	0.26	0.06	0.11	-0.06	-0.12
$dL/dt$ 1990-2009/11	0.13	0.17	<b>0.69</b>	1	<b>0.35</b>	<b>0.70</b>	<b>0.41</b>	<b>-0.40</b>	-0.32	<b>0.43</b>	0.26	0.22	<b>0.47</b>	-0.17	<b>0.49</b>	0.24	0.09	-0.02	-0.09	-0.01
Relative $dL$ Max-2009/11	<b>0.79</b>	<b>0.41</b>	<b>0.5450</b>	<b>0.35</b>	1	<b>0.69</b>	0.12	<b>0.38</b>	<b>0.56</b>	0.25	<b>0.49</b>	0.20	-0.20	<b>0.34</b>	0.20	0.15	<b>-0.62</b>	-0.18	0.15	0.20
Relative $dL$ 1990-2009/11	<b>0.54</b>	<b>0.58</b>	<b>0.36</b>	<b>0.70</b>	<b>0.69</b>	1	<b>0.37</b>	0.19	<b>0.42</b>	0.22	<b>0.39</b>	0.12	-0.21	0.26	0.09	0.06	<b>-0.45</b>	-0.23	0.05	0.24
$dH/dt$	<b>0.21</b>	0.08	0.15	<b>0.41</b>	0.12	<b>0.37</b>	1	<b>-0.48</b>	-0.33	-0.02	0.02	<b>0.72</b>	<b>0.69</b>	<b>0.31</b>	<b>0.67</b>	<b>0.74</b>	<b>0.41</b>	0.02	0.00	<b>0.25</b>

## 5 Discussion

In agreement with earlier studies from Svalbard (Kohler et al., 2007; Nuth et al., 2007; 2010; 2013; James et al., 2012), climate warming is anticipated to be the main control for the observed negative glacier changes in DL. Air temperature at the nearest meteorological station, SVL, clearly increased in the 1920s and 1930s, as well as after 1990 (Nordli et al., 2014), which explains the glacier retreat after the LIA maximum and in the last study epoch, respectively. However, clear post-1960 mass loss acceleration of DL glaciers may not simply be explained by increased air temperature. In the period 1960–1990 the total glacier area loss rate quadrupled (although with large uncertainty) and front retreat rates doubled, despite the fact that the mean multi-decadal summer air temperature was very similar to that in the first epoch and no decrease in winter snow accumulation over Svalbard was evident at that time (Pohjola et al., 2001; Hagen et al., 2003). In this context, it seems likely that average summer air temperature is not the only driver of change for small, low-activity glaciers in DL and other factors may also play a role. These could be, for example, different response times of glaciers or albedo feedbacks, which could modify glacier mass balance in a non-linear pattern,

1 e.g. by removal of high-albedo firn from accumulation zones and hence increase energy  
2 absorption (Kohler et al., 2007; James et al., 2012, Małecki 2013b).

3  
4 For the majority of glaciers in DL, the post-1990 period was marked by their fastest multi-  
5 decadal front retreat rates since the LIA maximum. This trend is similar to that on many land-  
6 terminating glaciers of Svalbard (Jania, 1988; Lankauf, 2007; Zagórski et al., 2008; James et  
7 al., 2012; Nuth et al., 2013) (Fig. 3). Length reduction was the main driver for glacier area  
8 decrease (Fig. 7b), which was high in DL and amounted to 37.9 %, supporting previous  
9 conclusions by Ziaja (2001) and Nuth et al. (2013) that central Spitsbergen, with its much  
10 smaller glaciers, is losing its ice cover extent at a relatively higher rate than maritime regions  
11 of Svalbard (e.g. 18 % area decrease in Sørkapp Land, 1936–1991, reported by Ziaja (2001)).  
12 Area loss rates in DL were at a similar level between 1960s–1990 and 1990–2009/11,  
13 comparable to the results in Nuth et al. (2013), who concluded there was no clear trend of  
14  $dA/dt$  evolution over the archipelago, except for southern Spitsbergen, where area loss rates  
15 generally decreased after 1990. On the other hand, Błaszczyk et al. (2013) concluded there  
16 were increasing area loss rates for tidewater glaciers in Hornsund, part of south Spitsbergen.  
17 Interestingly, ca. 800 km<sup>2</sup> of glaciers in Hornsund, often considered to be among the most  
18 sensitive to climate warming, have been losing area at a rate comparable to ca. 200 km<sup>2</sup> of  
19 small glaciers in DL (ca. 1 km<sup>2</sup> a<sup>-1</sup> for the period LIA–2000's).

20  
21 Clear acceleration of length loss rates indicates that glaciers in DL have been experiencing an  
22 increasingly negative mass balance since the termination of the LIA. This is in line with  
23 earlier studies. For seven glaciers in DL-C, Małecki (2013b) documented mean  $dH/dt$  of  
24  $-0.49$  m a<sup>-1</sup> for the period 1960s–1990, followed by an acceleration of mass loss rate to  $-0.78$   
25 m a<sup>-1</sup> after 1990. Kohler et al. (2007) analysed  $dH/dt$  of two small land-terminating glaciers in  
26 Spitsbergen with greater temporal resolution than that available for this study and concluded  
27 there was a continuous acceleration of their thinning over the 20<sup>th</sup> century, e.g. from  $dH/dt =$   
28  $-0.15$  m a<sup>-1</sup> (1936–1962) to  $dH/dt = -0.69$  m a<sup>-1</sup> (2003–2005) for Midre Lovénbreen in NW  
29 Spitsbergen. James et al. (2012) documented negative  $dH/dt$  for six small land-terminating  
30 glaciers all over Svalbard since at least the 1960s and reported a post-1990 increase in mass  
31 loss rates for four of these. Their recent  $dH/dt$  ranged from  $-0.28$  to  $-1.21$  m a<sup>-1</sup>, i.e. similar  
32 to the values observed in DL.

33  
34 An important finding of this study is the observation of the glacier-wide character of thinning  
35 over DL up to an elevation of 1000 m a.s.l., where the average 1990–2011 zero elevation  
36 change line was found. To put this into historical context, previous analyses performed for the  
37 earlier period 1960s–1990 identified this threshold at a much lower average altitude, i.e. at ca.  
38 600 m a.s.l. in DL-C (Małecki, 2013b; Małecki et al., 2013) (Fig. 6). The shift of the geodetic  
39 equilibrium suggests a recent negative change in glacier mass balance, including former  
40 accumulation zones. This hypothesis is supported by direct records (2011–2015) from  
41 Svenbreen (DL-C), where negative surface mass balance has also been noted at the highest  
42 ablation stake (625 m a.s.l.) near the glacier headwalls (Małecki, unpublished data). On  
43 Nordenskiöldbreen, a large tidewater glacier neighbouring DL from the east, mean 1989–  
44 2010 ELA, was modelled at 719 m a.s.l., i.e. higher than the accumulation zones of most DL  
45 glaciers (Van Pelt et al., 2012).

46  
47 Thinning at the high elevations of the study glaciers could be linked to several factors. Firstly,  
48 there is the increased melt energy availability due to: (i) increased incoming longwave  
49 radiation from the atmosphere and turbulent heat fluxes resulting from post-1990 summer air  
50 temperature rise, (ii) increased energy absorption by the ice surface due to decreasing albedo



1 caused by firn melt-out, dust or sediment delivery from freshly exposed headwalls and (iii)  
2 increased longwave emission from surrounding slopes recently uncovered from snow and ice.  
3 Other possible explanations are related to firn evolution, i.e. its compaction or melt-out,  
4 supporting the reduction of internal meltwater refreezing. The last probable mechanism could  
5 be a recent snow accumulation decrease. Data availability on winter mass balance in DL is  
6 insufficient for such conclusions (Troicki, 1988; Małeckki, 2015), but the trend for a snow  
7 precipitation decrease after 1990 has been noted for SVL station (James et al., 2012). Glacier  
8 dynamics could also be considered to be an explanation for changes in the glaciers' upper  
9 zones, but sparse data limit the interpretation possibilities. However, low flow velocities of  
10 DL glaciers ( $1\text{--}10\text{ m a}^{-1}$ ) suggest the minor importance of the dynamic component in their  
11 surface elevation changes.

12  
13 High-elevation glacier thinning in DL will have important consequences for the local  
14 cryosphere. Surge-type glaciers will not build up towards new surges and as such could be  
15 removed from the surge-cycle under present climate conditions, as demonstrated in more  
16 detail for Hørbyebreen by Małeckki et al. (2013). This will also lead to decay of temperate ice  
17 zones, still found beneath the largest glaciers of DL (Małeckki, unpublished data), and  
18 consequently it will influence their hydrology, geomorphological activity and reduce ice flow  
19 dynamics, as documented for other small glaciers in central Spitsbergen (Hodgkins et al.,  
20 1999; Lovell et al., 2015). Eventually, given that the highest parts of glaciers in DL typically  
21 reach 700–800 m a.s.l., the high altitude of the recent geodetic equilibrium suggests their  
22 considerable or complete melt-out in the future, even if the atmospheric warming trend has  
23 stopped. Notably, altitude had the strongest influence on the spatial mass balance variability  
24 (Figs. 6 and 7a), so small low-elevated glaciers were the most sensitive to climate shift. They  
25 had the fastest front retreat rates and the most negative  $dH/dt$  (Fig. 7a); hence, they are likely  
26 to be the first to disappear.

27  
28 Glacier-wide surface lowering has already been triggered in some of the world's largest ice  
29 repositories, including the Canadian Arctic Archipelago (Gardner et al., 2011) and Patagonian  
30 icefields (Willis et al., 2012), causing them to significantly contribute to sea-level rise. In  
31 Svalbard, the major ice masses are still building up their higher zones and remain closer to  
32 balance (Moholdt et al., 2010; Nuth et al., 2010), but the process of high-elevation thinning  
33 seems to be already widespread on smaller glaciers across the archipelago, as documented by  
34 Kohler et al. (2007), James et al. (2012) and confirmed by this study. By the end of the 21<sup>st</sup>  
35 century, a further 3–8°C warming over Svalbard is predicted by climate models (Førland et  
36 al., 2011; Lang et al., 2015). This will eventually cause the complete decay of the  
37 accumulation zones of Svalbard ice masses, boosting their mass loss rates and the sea-level  
38 rise contribution from the region. Small Spitsbergen glaciers may, therefore, be perceived as  
39 an early indicator of the future changes of larger ice caps and icefields.

40  
41 The mass balance of glaciers in central Spitsbergen has been previously considered by some  
42 researchers as relatively resistant to climate change due to the prevailing dry conditions and  
43 high hypsometry (Nuth et al., 2007). However, at  $-0.71 \pm 0.05\text{ m a}^{-1}$  ( $-0.64 \pm 0.05\text{ m w.e.}$   
44  $\text{a}^{-1}$ ) the average mass balance of glaciers in DL is among the most negative of the Svalbard  
45 regional means reported by Nuth et al. (2010) and Moholdt et al. (2010). Previously published  
46 occasional data from another region of central Spitsbergen, Nordenskiöld Land, shows a  
47 generally similar glacier response to climate change and comparable mass balances to glaciers  
48 in DL (e.g. Troicki, 1988; Ziaja and Pipała, 2007; Bælum and Benn, 2011), indicating that  
49 observations from this study are valid for larger areas of the island's interior. Extrapolation of  
50 the mass balance from DL to glaciers in eastern DL-C and to neighbouring Nordenskiöld

1 Land and Bünsow Land (Fig. 1a), comparable in terms of climate and glacier-cover  
2 characteristics, yields an estimate of the total mass balance of glaciers in central Spitsbergen.  
3 Despite their negligible share of the archipelago's ice area (ca. 800 km<sup>2</sup> or 2 %), they  
4 contribute about 0.6 Gt a<sup>-1</sup> to the sea-level rise, a figure comparable to the contribution of  
5 some of the much larger glacier regions, e.g. parts of southern or eastern Svalbard. The total  
6 mass balance of the archipelago has been estimated to range from -4.3 Gt a<sup>-1</sup> (Moholdt et al.,  
7 2010) to -9.7 Gt a<sup>-1</sup> (Nuth et al., 2010).

## 10 **6 Conclusions**

12 In this study, a multi-temporal inventory and digital elevation models of 152 small alpine  
13 glaciers and ice patches in Dickson Land, central Spitsbergen, were used to document their  
14 post-Little Ice Age evolution. In order to be in balance with the present climate, their ELA  
15 should be approximately 500 m a.s.l. However, due to progressive climate warming in  
16 Svalbard, the average ELA migrated much higher and glaciers have been continuously losing  
17 mass for many decades. The total ice area in Dickson Land has been declining at an  
18 accelerating rate from 334.1 ± 38.4 km<sup>2</sup> at the termination of the Little Ice Age (early 20<sup>th</sup>  
19 century) to 207.4 ± 4.6 km<sup>2</sup> in 2009/11, corresponding to an overall 37.9 ± 12.1 % decrease.  
20 Post-1990 area loss rate was 4.5 times higher than in the epoch LIA-1960's, i.e. 2.23 ± 0.48  
21 km<sup>2</sup> a<sup>-1</sup> vs. 0.49 ± 0.66 km<sup>2</sup> a<sup>-1</sup>, respectively. Front retreat of 66 test-glaciers has accelerated  
22 over time, i.e. from an average of 4.9 ± 0.1 m a<sup>-1</sup> in the period from the Little Ice Age  
23 maximum to the 1960s, 9.4 ± 0.1 m a<sup>-1</sup> between the 1960s and 1990, to 16.4 ± 0.1 m a<sup>-1</sup> in  
24 the last study epoch 1990-2009/11, which turned out to be the period of the fastest retreat for  
25 74 % of glaciers.

27 The most important finding of this study is the recent rapid glacier-wide thinning over the  
28 entire region at a mean rate of 0.71 ± 0.05 m a<sup>-1</sup> (-0.64 ± 0.05 m w.e. a<sup>-1</sup>). The warming  
29 climate has caused an ELA rise and a consequent increase in the zero-elevation change line,  
30 so local glaciers have been thinning up to the altitude of 1000 m, i.e. higher than their  
31 accumulation zones. This shift will eventually lead to the complete melt-out of most of the  
32 study glaciers, even if the observed climate warming stops. The spatial variability of glacier  
33 mass balance was primarily correlated with elevation, so small low-elevated glaciers have  
34 generally been losing mass and length at the fastest rates and are under threat of the earliest  
35 disappearance. Application of the mean specific mass balance calculated for Dickson Land to  
36 two other regions of central Spitsbergen, very similar in terms of climate and glacier-cover,  
37 yields an estimate of the total mass balance of small glaciers in the dry interior of Spitsbergen  
38 of -0.6 Gt a<sup>-1</sup>, a figure which should be considered in future assessments of the contribution  
39 of Svalbard to sea-level rise.

## 42 **Acknowledgements**

44 The study is a contribution to the DIL\*ICE project (Dickson Land Ice Masses Evolution, RiS  
45 id 4894) supported by the Polish National Science Centre (grant N N306 062940) and the  
46 Institute of Geocology and Geoinformation of Adam Mickiewicz University in Poznań. The  
47 author sincerely appreciates the support from Copernicus Publications and the open-access  
48 data policy of the Norwegian Polar Institute. Constructive reviews from P. Holmlund and J.  
49 Kohler helped to significantly improve the manuscript and are greatly appreciated. The  
50 comments of J.O. Hagen on the early manuscript are also acknowledged.



## References

- Bælum, K., and Benn, D.I. 2011. Thermal structure and drainage system of a small valley glacier (Tellbreen, Svalbard), investigated by ground penetrating radar. *The Cryosphere*, 5, 139-149, 2011.
- Błaszczyk, M., Jania, J., and Kolondra, L.: Fluctuations of tidewater glaciers in Hornsund Fjord (Southern Svalbard) since the beginning of the 20<sup>th</sup> century. *Pol. Polar Res.*, 34, 327-352, 2013.
- Cox, L.H., and March, R.S.: Comparison of geodetic and glaciological mass-balance techniques, Gulkana Glacier, Alaska, U.S.A. *J. Glaciol.* 50, 363–370, 2004.
- Evans, D.J.A., Strzelecki, M., Milledge, D.G., and Orton, C.: Hørbyebreen polythermal glacial system, Svalbard. *Journal of Maps*, 8, 146-156, 2012.
- Ewertowski, M.: Recent transformations in the high-Arctic glacier landsystem, Ragnarbreen, Svalbard. *Geogr. Ann. A*, 93, 265-285, 2014. doi:10.1111/geoa.12049
- Ewertowski, M., and Tomczyk, A.: Quantification of the ice-cored moraines' short-term dynamics in the high-Arctic glaciers Ebbabreen and Ragnarbreen, Petuniabukta, Svalbard. *Geomorphology* 234, 211-227, 10.1016/j.geomorph.2015.01.023, 2015.
- Ewertowski, M., Kasprzak, L., Szuman, I., and Tomczyk, A.M.: Depositional processes within the frontal ice-cored moraine system, Ragnar glacier, Svalbard. *Quaestiones Geographicae*, 29, 27-36, 2010.
- Ewertowski, M., Kasprzak, L., Szuman, I., and Tomczyk, A.M.: Controlled, ice-cored moraines: sediments and geomorphology. An example from Ragnarbreen, Svalbard. *Z. Geomorphol.*, 51, 53-74. doi: 10.1127/0372-8854/2011/0049, 2012.
- Fischer, M., Huss, M., and Hoelzle, M.: Surface elevation and mass changes of all Swiss glaciers 1980–2010. *The Cryosphere*, 9, 525–540, 2015.
- Førland, E. J., Benestad, R., Hanssen-Bauer, I., Haugen, J. E., and Skaugen, T. E.: Temperature and Precipitation Development at Svalbard 1900–2100, *Advances in Meteorology*, 2011, 893790, doi:10.1155/2011/893790, 2011.
- Gardner, A.S., Moholdt, G., Wouters, B., Wolken, G.J., Burgess, D.O., Sharp, M.J., Cogley, J.G., Braun, C. and Labine, C. 2011. Sharply increased mass loss from glaciers and ice caps in the Canadian Arctic Archipelago. *Nature*, 473, 357-360, 2011.
- Gardner, A.S., Moholdt, G., Cogley, J.G., Wouters, B., Arendt, A.A., Wahr, J., Berthier, E., Hock, R., Pfeffer, W.T., Kaser, G., Ligtenberg, S.R.M., Bolch, T., Sharp, M.J., Hagen, J.O., van den Broecke, M.R., and Paul, F.: A reconciled estimate of glacier contributions to sea level rise: 2003 to 2009, *Science*, 340, 852–857, 2013.
- Gibas, J., Rachlewicz, G., and Szczuciński, W.: Application of DC resistivity soundings and geomorphological surveys in studies of modern Arctic glacier marginal zones, Petuniabukta, Spitsbergen. *Pol. Polar Res.* 26, 239–258, 2005.
- Hagen, J.O., Liestøl, O., Roland, E., and Jørgensen, T.: *Glacier atlas of Svalbard and Jan Mayen*. Oslo: Norwegian Polar Institute, 1993.
- Hagen, J.O., Kohler, J., Melvold, K., and Winther, J.-G.: Glaciers in Svalbard: mass balance, runoff and freshwater flux. *Polar Res.*, 22, 145–159, 2003.
- Hodgkins, R., Hagen, J.O. and Hamran, S.-E.: 20<sup>th</sup> century mass balance and thermal regime change at Scott Turnerbreen, Svalbard. *Ann. Glaciol.*, 28, 216-220.
- IPCC: *Climate Change 2013, The Physical Science Basis, Working Group I Contribution to the Fifth Assessment Report of the Intergovernmental Panel on Climate Change*, WMO / UNEP, Cambridge University Press, Geneva, 2013.

- 1 James, T.D., Murray, T., Barrand, N.E., Sykes, H.J., Fox, A.J., and King, M.A.: Observations  
2 of enhanced thinning in the upper reaches of Svalbard glaciers. *The Cryosphere*, 6, 1369-  
3 1381, 2012.
- 4 Jania, J.: Dynamiczne procesy glacialne na południowym Spitsbergenie w świetle badań  
5 fotointerpretacyjnych i fotogrametrycznych (Dynamic glacial processes in south  
6 Spitsbergen in the light of photointerpretation and photogrammetry). *Prace Naukowe*  
7 *Uniwersytetu Śląskiego*, Katowice, ISBN 83-226-0200-6, 1988.
- 8 Karczewski, A.: The development of the marginal zone of the Hørbyebreen, Petuniabukta,  
9 central Spitsbergen. *Pol. Polar Res.*, 10, 371-377, 1989.
- 10 Kohler, J., James, T. D., Murray, T., Nuth, C., Brandt, O., Barrand, N. E., Aas, H. F., and  
11 Luckman, A.: Acceleration in thinning rate on western Svalbard glaciers. *Geophys. Res.*  
12 *Lett.*, 34, L18502, doi 10.1029/2007GL030681, 2007.
- 13 Kostrzewski, A., Kaniecki, A., Kapuściński, J., Klimczak, R., Stach, A., and Zwoliński, Z.:  
14 The dynamics and rate of denudation of glaciated and non-glaciated catchments, central  
15 Spitsbergen. *Pol. Polar Res.*, 10, 317-367, 1989.
- 16 König, M., Kohler, J. and Nuth, C.: Glacier Area Outlines - Svalbard. Norwegian Polar  
17 Institute (Tromsø, Norway): [https://data.npolar.no/dataset/89f430f8-862f-11e2-8036-](https://data.npolar.no/dataset/89f430f8-862f-11e2-8036-005056ad0004)  
18 [005056ad0004](https://data.npolar.no/dataset/89f430f8-862f-11e2-8036-005056ad0004), 2013.
- 19 Lang, C., Fettweis, X., and Erpicum, M.: Future climate and surface mass balance of Svalbard  
20 glaciers in an RCP8.5 climate scenario: a case study with the regional climate model  
21 MAR forced by MIROC5. *The Cryosphere*, 9, 945-956, 2015.
- 22 Lankauf, K.R.: Recesja lodowców rejonu Kaffiøyry (Ziemia Oskara II - Spitsbergen) w XX  
23 wieku (Retreat of Kaffiøyra glaciers [Oscar II Land – Spitsbergen] in the 20<sup>th</sup> century).  
24 *Prace Geograficzne nr. 183*, Polska Akademia Nauk, Warszawa, 2002.
- 25 Láska, K., Witoszová, D., and Prošek, P.: Weather patterns of the coastal zone of  
26 Petuniabukta, central Spitsbergen in the period 2008-2010. *Pol. Polar Res.*, 33, 297-318,  
27 2012.
- 28 Li, Ya., and Li, Yi.: Topographic and geometric controls on glacier changes in the central  
29 Tien Shan, China, since the Little Ice Age. *Ann. Glaciol.*, 55, 177-186, 2014 doi:  
30 10.3189/2014AoG66A031, 2014.
- 31 Lovell, H., Fleming, E.J., Benn, D.I., Hubbard, B., Lukas, S. and Naegeli, K.: Former  
32 dynamic behaviour of a cold-based valley glacier on Svalbard revealed by basal ice and  
33 structural glaciology investigations. *J. Glaciol.*, 61, 309-328, 2015.
- 34 Małecki, J.: The present-day state of Svenbreen (Svalbard) and changes of its physical  
35 properties after the termination of the Little Ice Age. PhD thesis, Adam Mickiewicz  
36 University in Poznań, pp. 145, 2013a.
- 37 Małecki, J.: Elevation and volume changes of seven Dickson Land glaciers, Svalbard. *Polar*  
38 *Res.*, 32, 18400, 2013b.
- 39 Małecki, J.: Some comments on the flow velocity and thinning of Svenbreen, Dickson Land,  
40 Svalbard. *Czech Polar Reports*, 4, 1-8, 2014.
- 41 Małecki, J.: Snow accumulation on a small high-Arctic glacier Svenbreen – variability and  
42 topographic controls. *Geogr. Ann. A.*, 97, 809-817, 2015.
- 43 Małecki, J., Faucherre, S., and Strzelecki, M.: Post-surge geometry and thermal structure of  
44 Hørbyebreen, central Spitsbergen. *Pol. Polar Res.* 34, 305-321, 2013.
- 45 Martín-Español, A., Navarro, F.J., Otero, J., Lapazaran, J.J., and Błaszczuk, M.: Estimate of  
46 the total volume of Svalbard glaciers, and their potential contribution to sea-level rise,  
47 using new regionally based scaling relationships. *J. Glaciol.*, 61,  
48 doi:10.3189/2015JoG14J159, 2015.

- 1 Moholdt, G., Nuth, C., Hagen, J.O., and Kohler, J.: Recent elevation changes of Svalbard  
2 glaciers derived from ICESat laser altimetry. *Remote Sens. Environ.*, 114, 2756-2767,  
3 2010.
- 4 Nordli, Ø., Przybylak, R., Ogilvie, A.E.J., and Isaksen, K.: Long-term temperature trends and  
5 variability on Spitsbergen: the extended Svalbard Airport temperature series, 1898-2012.  
6 *Polar Res.* 33, 21348, doi:<http://dx.doi.org/10.3402/polar.v33.21349>, 2014.
- 7 Norwegian Polar Institute: Kartdata Svalbard 1:100 000 (S100 Kartdata). Tromsø, Norway:  
8 Norwegian Polar Institute. <https://data.npolar.no/dataset/645336c7-adfe-4d5a-978d-9426fe788ee3>, accessed 2<sup>nd</sup> January 2015, 2014a.
- 9  
10 Norwegian Polar Institute: Terrengmodell Svalbard (S0 Terrengmodell). Tromsø, Norway:  
11 Norwegian Polar Institute. <https://data.npolar.no/dataset/dce53a47-c726-4845-85c3-a65b46fe2fea>, accessed 3<sup>rd</sup> March 2015, 2014b.
- 12  
13 Nuth, C., and Kääb, A.: Co-registration and bias corrections of satellite elevation data sets for  
14 quantifying glacier thickness change. *The Cryosphere*, 5, 271-290, 2011.
- 15 Nuth, C., Kohler, J., Aas, H.F., Brandt, O., and Hagen, J.O.: Glacier geometry and elevation  
16 changes on Svalbard (1936– 90): a baseline dataset. *Ann. Glaciol.*, 46, 106-116, 2007.
- 17 Nuth, C., Moholdt, G., Kohler, J., Hagen, J. O., and Kääb, A.: Svalbard glacier elevation  
18 changes and contribution to sea level rise. *J. Geophys. Res.*, 115, F01008, doi  
19 10.1029/2008JF001223, 2010.
- 20 Nuth, C., Kohler, J., König, M., von Deschanden, A., Hagen, J.O., Kääb, A., Moholdt, G.,  
21 and Pettersson, R.: Decadal changes from a multi-temporal glacier inventory of Svalbard.  
22 *The Cryosphere*, 7, 1603–1621, 2013.
- 23 Oerlemans, J.: Extracting a Climate Signal from 169 Glacier Records, *Science*, 308, 675–677,  
24 doi:10.1126/science.1107046, 2005.
- 25 Paul, F., and Mölg, N.: Hasty retreat of glaciers in northern Patagonia from 1985 to 2011. *J.*  
26 *Glaciol.*, Vol. 60, No. 224, 2014 doi: 10.3189/2014JoG14J104, 2014.
- 27 Pleskot, K.: Sedimentological characteristics of debris flow deposits within ice-cored  
28 moraine of Ebbabreen, central Spitsbergen. *Pol. Polar Res.*, 36, 125-144, 2015.
- 29 Pohjola, V.A., Martma, T., Meijer, H.A.J., Moore, J.C., Isaksson, E., Vaikmae, R., and van de  
30 Wal, R.S.W.: Reconstruction of three centuries of annual accumulation rates based on the  
31 record of stable isotopes of water from Lomonosovfonna, Svalbard. *Ann. Glaciol.*, 35, 57-  
32 62, 2002.
- 33 Przybylak, R., Arażny, A., Nordli, Ø., Finkelnburg, R, Kejna, M., Budzik, T., Migala, K.,  
34 Sikora, S., Puczko, D., Rymer, K., and Rachlewicz, G.: Spatial distribution of air  
35 temperature on Svalbard during 1 year with campaign measurements. *Int. J. Climatol.*, 34,  
36 3702-3719, 2014. DOI: 10.1002/joc.3937, 2014.
- 37 Rachlewicz, G.: River floods in glacier-covered catchments of the high Arctic: Billefjorden-  
38 Wijdefjorden, Svalbard. *Norsk Geogr. Tidskr.*, 63, 115-122, 2009a.
- 39 Rachlewicz, G.: Contemporary sediment fluxes and relief changes in high Arctic glacierized  
40 valley systems (Billefjorden, Central Spitsbergen). *Uniwersytet im. Adama Mickiewicza*  
41 *w Poznaniu, seria geografia nr 87. Poznań, Poland: Wydawnictwo Naukowe UAM,*  
42 2009b.
- 43 Rachlewicz, G., and Styszyńska, A.: Porównanie przebiegu temperatury powietrza w  
44 Petuniabukta i Svalbard-Lufthavn (Isfjord, Spitsbergen) w latach 2001-2003. (Comparison  
45 of the course of air temperature in Petuniabukta and Svalbard-Lufthavn (Isfjord,  
46 Spitsbergen) in the years 2001-2003.) *Problemy Klimatologii Polarnej* 17, 121-134, 2007.
- 47 Rachlewicz, G., Szczuciński, W., and Ewertowski, M.: Post -"Little Ice Age" retreat rates of  
48 glaciers around Billefjorden in central Spitsbergen, Svalbard. *Pol. Polar Res.*, 28, 159-186,  
49 2007.

- 1 Radić, V., and Hock, R.: Regionally differentiated contribution of mountain glaciers and ice  
2 caps to future sea-level rise. *Nat. Geosci.*, 4, 91–94, 2011.
- 3 Strzelecki, M.C., Małecki, J., Zagórski, P.: The influence of recent deglaciation and  
4 associated sediment flux on the functioning of polar coastal zone - northern Petuniabukta,  
5 Svalbard. [In:] *Sediment Fluxes in Coastal Areas*. Coastal Research Library 10, M.  
6 Maanan, M. Robin (eds.), Springer Science+Business Media, Dordrecht: 23-45, ISBN  
7 978-94-017-9259-2, 2015a.
- 8 Strzelecki, M.C., Long, A.J., Lloyd, J.M.: Post-Little Ice Age development of a High Arctic  
9 paraglacial beach complex. *Permafrost Periglac.*, DOI: 10.1002/ppp.1879, 2015b.
- 10 Sobota, I.: Selected methods in mass balance estimation of Waldemar Glacier, Spitsbergen.  
11 *Pol. Polar Res.*, 28, 249-268, 2007.
- 12 Szpikowski, J., Szpikowska, G., Zwoliński, Z., Rachlewicz, G., Kostrzewski, A., Marciniak,  
13 M., and Dragon, K.: Character and rate of denudation in a High Arctic glacierized  
14 catchment (Ebbaelva, Central Spitsbergen). *Geomorphology*, 218, 52-62, 2014.  
15 <http://dx.doi.org/10.1016/j.geomorph.2014.01.012>, 2014.
- 16 Szczuciński, W., Zajączkowski, M., and Scholten J.: Sediment accumulation rates in subpolar  
17 fjords – Impact of post-Little Ice Age glaciers retreat, Billefjorden, Svalbard. *Estuar.  
18 Coast. Shelf S.*, 85, 345-356, 2009.
- 19 Troicki, L.S.: O balance massy lednikov raznyh tipov na Špicbergenie (On the mass balance  
20 of different types of glaciers on Spitsbergen). *Materialy Glyaciologičeskikh Issledovanij*,  
21 63, 117-121, 1988.
- 22 Van Pelt, W.J.J., Oerlemans, J., Reijmer, C.H., Pohjola, V.A., Pettersson, R., and Angelen,  
23 J.H.: Simulating melt, runoff and refreezing on Nordenskiöldbreen, Svalbard, using a  
24 coupled snow and energy balance model. *The Cryosphere*, 6, 641-659, 2012.
- 25 Willis, M.J., Melkonian, A.K., Pritchard, M.E. and Rivera, A.: Ice loss from the Southern  
26 Patagonian Ice Field, South America, between 2000 and 2012. *Geophys. Res. Lett.*, 39,  
27 L17501, 2012.
- 28 Zagórski, P., Siwek, K., Gluza, A., and Bartoszewski, S.A.: Changes in the extent and  
29 geometry of the Scott Glacier, Spitsbergen. *Pol. Polar Res.*, 29, 163-185, 2008.
- 30 Ziaja, W.: Glacial recession in Sørkappland and central Nordenskiöldland, Spitsbergen,  
31 Svalbard, during the 20<sup>th</sup> century. *Arct. Antarct. Alp. Res.*, 33, 36-41, 2001.
- 32 Ziaja, W. and Pipała, R.: Glacial recession 2001-2006 and its landscape effects in the  
33 Lindströmfjellet-Håbergnuten mountain ridge, Nordenskiöld Land, Spitsbergen. *Pol. Polar  
34 Res.*, 28, 237-247, 2007.
- 35 Žuravlev, A.B., Mačeret, Ju.Ja., and Bobrova, L.I.: Radiolokaličjonnije issledovanije na  
36 poljarnom lednike s zimnym stokom (Radio-echo sounding investigations on a polar  
37 glacier with winter discharge). *Materialy Glyaciologičeskikh Issledovanij*, 46, 143-149,  
38 1983.